Noname manuscript No.
(will be inserted by the editor)

On spherical harmonics based numerical quadrature over the surface of a sphere

Bengt Fornberg · Jordan M. Martel

the date of receipt and acceptance should be inserted later

Keywords Quadrature, Sphere, Spherical Harmonics, ME nodes, MD nodes, Gaussian Quadrature.

Mathematics Subject Classification (2000) 65D30, 65D32, 41A55.

Abstract It has been suggested in the literature that different quasi-uniform node sets on a sphere lead to quadrature formulas of highly variable quality. We analyze here the nature of these variations, and describe an easy-to-implement least-squares remedy for previously problematic cases. Quadrature accuracies are then compared for different node sets ranging from fully random to those based on Gaussian quadrature concepts.

1 Introduction

Numerous applications require computations over spherical surfaces. Often, such calculations need to be supplemented by evaluations of various globally integrated quantities, such as total energy, average temperature, etc., necessitating the supplementary step of numerical quadrature. In case the computation is carried out in the space of spherical harmonics (SPH), the global surface integral is immediately available as the coefficient of the constant zero$^{\text{th}}$ mode (since all other SPH modes are orthogonal to this one, and thus integrate to zero). However, scattered nodes together with radial basis function (RBF) based discretizations have recently been found to be highly effective for solving PDEs in this geometry (Fornberg and Piret,

Bengt Fornberg
Department of Applied Mathematics
University of Colorado at Boulder
Boulder, CO 80309
E-mail: fornberg@colorado.edu

Jordan M. Martel
Leeds School of Business
University of Colorado at Boulder
Boulder, CO 80309
E-mail: jordan.martel@colorado.edu

2008; Fornberg and Lehto, 2011), especially in the context of geophysical flows as surveyed in Flyer and Fornberg (2011) and Flyer et al. (2012, 2014), renewing the question of finding good quadrature weights for semi-uniform node sets over spherical surfaces.

The only instances of fully uniform node sets on a sphere are given by the N vertices of the five Platonic bodies, with $N = 4$, 6, 8, 12, and 20, respectively. In these cases, the optimal quadrature weights are all the same; for the unit sphere $w_i = 4\pi/N$, $i = 1, \ldots, N$. In most applications, very much higher resolution is needed than what can be provided by $N = 20$ nodes. Quadrature weights have therefore been tabulated for some types of near-uniform node distributions, extending to much higher values for N (Womersley and Sloan, 2001, 2003). In analogy to how weights in 1-D often are determined by requiring exact results for polynomials of high degrees, weights for the sphere were there obtained by requiring exact quadrature results for as high order spherical harmonics (SPH) as possible. It was then found that certain near-uniform node configurations work much better than others. In particular, Minimal Energy (ME) nodes – corresponding to equilibria of mutually repelling particles – were found to lead to very inaccurate quadrature approximations. Therefore, Maximal Determinant (MD) node sets were constructed by instead optimizing the conditioning of SPH interpolation. Quadrature based on SPH interpolation was consequently described as a “sometimes dangerous strategy” in Hesse et al. (2010). The present work is motivated by our observation that this “danger” is avoidable, and that excellent quadrature weights can be reliably computed also for ME node sets.

After noting in Section 2 that the key issue with regard to calculating quadrature weights via SPH expansions is to avoid *rank deficiency*, we describe in Section 3 a least squares approach that overcomes this by means of slightly reducing the order of SPH that are considered. To put the MD vs. ME quadrature results in a somewhat wider context, the test results in Section 4 include also very irregular node sets (Random and Halton) and a highly regular one – a Gaussian-type quadrature method for the sphere developed by Ahrens and Beylkin (2009).

2 Conceptual flaw with immediate SPH-based interpolation

We summarize in this section the relation between SPH and quadrature weights, and note why an immediate SPH interpolation is likely to give quadrature weights of erratic quality.

2.1 Connection between SPH and numerical quadrature

As alluded to in the Introduction, the most direct strategy for finding quadrature weights w_i at nodes $\underline{x}_i$, $i = 1, 2 \ldots, N = (m+1)^2$ on the unit sphere is to require that $\sum_{i=1}^{N} w_i f_i$ evaluates to the correct surface integral whenever the node data f_i is any combination $\sum_{i=1}^{N} \lambda_i \psi_i(\underline{x})$ of the N first SPH basis functions $\{\psi_i(\underline{x}),\ i =$

$1, 2, \ldots, N\}$, i.e.

$$\overbrace{\begin{bmatrix} \psi_1(\underline{x}_1) & \psi_2(\underline{x}_1) & \cdots & \psi_N(\underline{x}_1) \\ \psi_1(\underline{x}_1) & \psi_2(\underline{x}_2) & \cdots & \psi_N(\underline{x}_2) \\ \vdots & \vdots & \ddots & \vdots \\ \psi_1(\underline{x}_N) & \psi_2(\underline{x}_N) & \cdots & \psi_N(\underline{x}_N) \end{bmatrix}}^{P} \begin{bmatrix} \lambda_1 \\ \lambda_2 \\ \vdots \\ \lambda_N \end{bmatrix} = \begin{bmatrix} f_1 \\ f_2 \\ \vdots \\ f_N \end{bmatrix}, \tag{1}$$

or briefer, $P\underline{\lambda} = \underline{f}$, implying $\underline{\lambda} = P^{-1}\underline{f}$ (for P invertible). A common way to represent the $N = (m+1)^2$ first SPH basis functions $\psi_i(\underline{x})$ is as $Y_\mu^\nu(\underline{x})$, where $\underline{x} = [x, y, z]$ with $||\underline{x}||_2 = 1$, degree $\mu = 0, 1, \ldots, m$ and order $\nu = -\mu, \ldots, 0, \ldots, +\mu$ (advancing by degrees, i.e. starting with $\psi_1(\underline{x}) = Y_0^0(\underline{x})$). They can be expressed as associated Legendre functions in z and trigonometric functions (either real or complex valued) angularly around the z-axis. Since they are scaled to become orthonormal, it will hold that

$$\int_{\text{sphere surface}} Y_\mu^\nu(\underline{x})\, dS = \begin{cases} 1\ , \ \mu = \nu = 0 \\ 0 \quad \text{otherwise} \end{cases} . \tag{2}$$

It now follows from (1), (2) that we can read off the SPH-generated quadrature weights w_i as the entries in the first row of P^{-1}.

2.2 A general observation about the use of node independent basis functions

Following a classical argument (Mairhuber, 1956; Curtis, 1959), we consider a scattered node set $\{\underline{x}_i,\ i = 1, 2, \ldots, N\}$ in R^d with associated data values $\{f_i,\ i = 1, 2, \ldots, N\}$, and an equally large set of basis functions $\{\psi_i(\underline{x}),\ i = 1, 2, \ldots, N\}$ (now no longer necessarily the SPH set). The condition for

$$s(\underline{x}) = \sum_{i=1}^{N} \lambda_i \psi_i(\underline{x}) \tag{3}$$

to interpolate the data becomes again $P\underline{\lambda} = \underline{f}$. If any two node locations $\underline{x}_i$ and $\underline{x}_j$ are moved in such way that they become interchanged, the two corresponding rows of the interpolation matrix P in (1) also become interchanged, i.e. $\det(P)$ has changed sign. By continuity, P must therefore have been singular somewhere along the way. In 1-D, such node interchanges are impossible if node locations are assumed to remain distinct, but there is no such limitation in higher dimensions. In particular, when interpolating using SPH, there will be vast numbers of visually plausible but nevertheless singular node distributions. As Figure 1 illustrates, MD node sets succeed (by their construction) to keep far away from these singular cases. Although ME node sets feature very uniform node distributions, their construction offers no protection against the ill-conditioning. Already tiny perturbations of node locations can in fact cause singularities. Figure 2 displays in a different way the near-singularity of a ME node set with regard to SPH interpolation, illustrating that it actually causes major in-between node oscillations in ME cases.

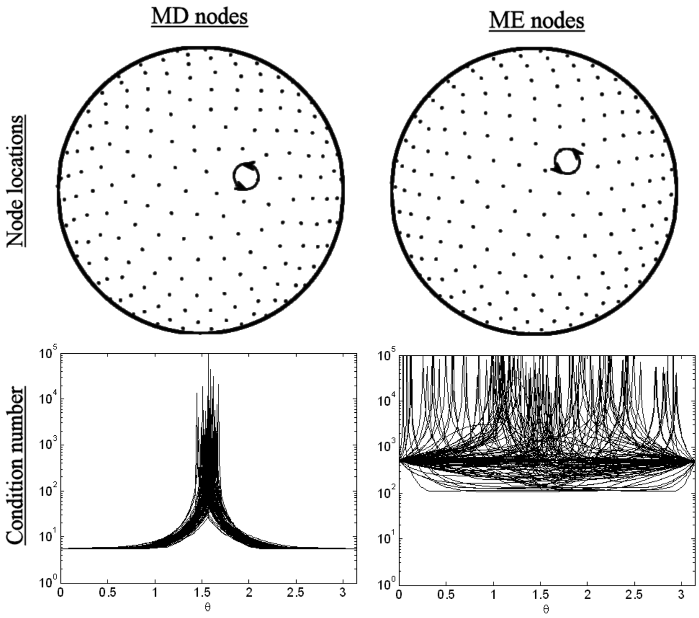

Fig. 1 Top row of subplots: Examples of $N = 400$ MD and ME node sets, also illustrating the idea of interchanging two adjacent nodes by a rotation around their midpoint. Bottom row of subplots: The condition number when 100 randomly selected such pairs of the nodes (separately) are rotated in this way, shown as function of the rotation angle θ.

To explore further the impact of node set details, we consider next five of the node sets shown in Figure 3 (delaying the discussion of the Gaussian quadrature GQ set until Section 4.3). The Halton (Halton, 1960) and random node sets are obtained from their counterparts in a $(t_i, z_i) \in [-1, 1] \times [-1, 1]$ square region case by the mapping

$$\begin{cases} x_i = \sqrt{1 - z_i^2}\cos(t_i\pi) \\ y_i = \sqrt{1 - z_i^2}\sin(t_i\pi) \\ z_i = z_i. \end{cases}$$

Figure 4 displays the singular values for the corresponding SPH interpolation matrices. The severe 'mismatch' between SPH representations and Latitude-Longitude grids is well known (Boyd, 2000). With regard to the difference between MD and ME node sets, we see that this affects only the very last singular values. This observation suggests our present approach for calculating quadrature weights, described in Section 3.

Node sets of 'cubed sphere' type have received quite extensive attention; see, for example, Flyer et al. (2012) for examples and computational comparisons. The cubed sphere idea is to radially project node sets from an inscribed cube to the sphere surface. Each cube face can for example be discretized in Gauss-Lobatto style, or partitioned into smaller squares, which then are discretized in this way. Figure 5, parts (a) and (b) show two such discretizations (when looking straight down on one of the cube faces), both when $N = 1352$ nodes. Part (c) shows that

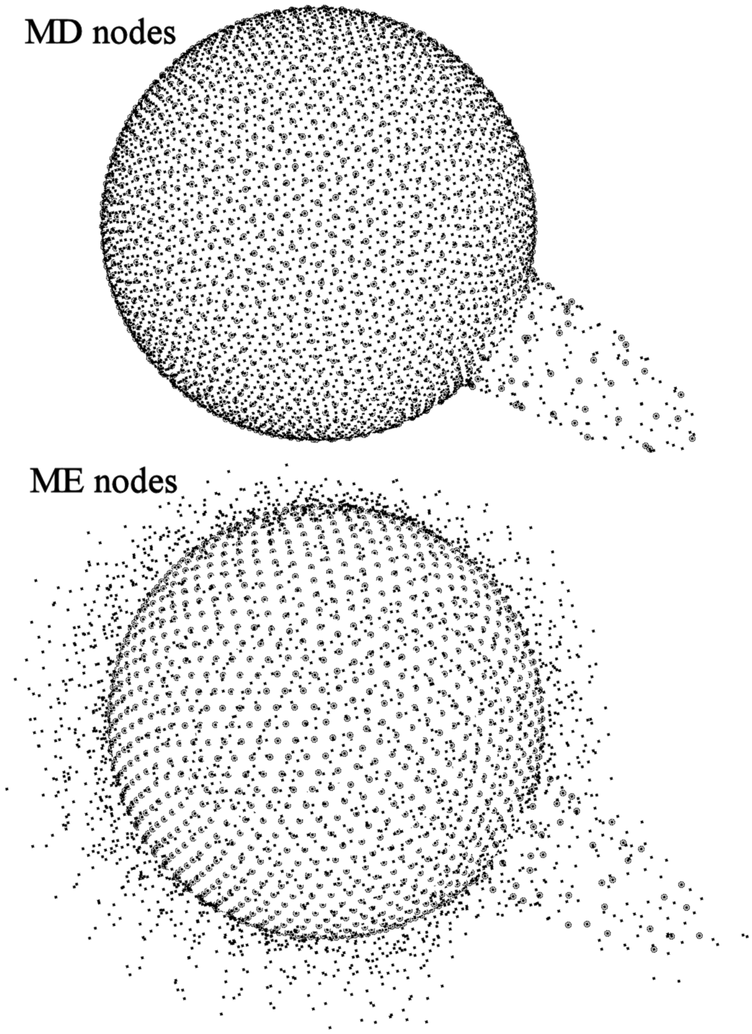

Fig. 2 A 'cosine bell' defined at $N = 1849$ MD and ME node points (small circular markers) with the SPH interpolants shown (as dots) at these as well as at numerous additional locations. Function values are represented by radial distances from the origin. With a sphere of unit radius, the bell has a height of 1 and at its base a radius of 1/3.

this leads to singular value distributions more reminiscent of Lat-Long node sets than of, say, MD and ME.

3 Calculation of quadrature weights based on omitting highest SPH degree(s)

In view of Figures 4 and 5, we will not consider Lat-Long grids or cubed spheres any further. With regard to the ME, Halton and Random node layouts, it is only the

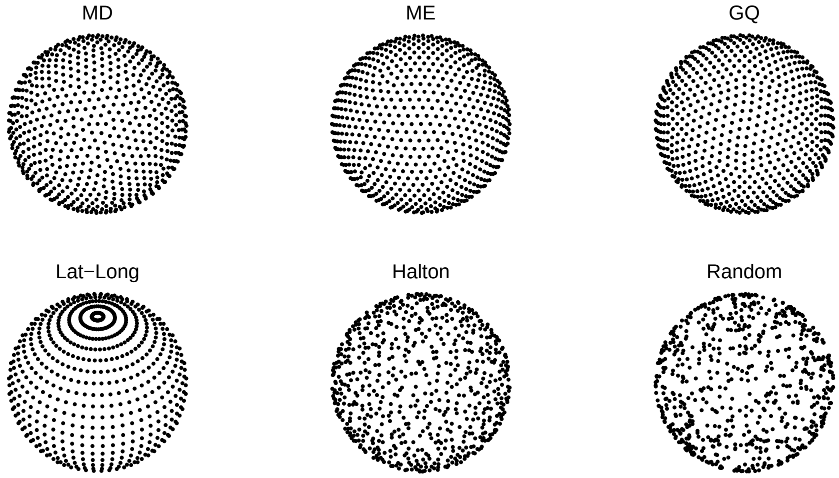

Fig. 3 Illustrations of six different node point distributions on the unit sphere (with $N = 1296$ nodes in all cases, apart from $N = 1332$ for the GQ case). The barely visible differences between the MD, ME and GQ cases are noteworthy, as they greatly affect the accuracy of immediate SPH interpolation and quadrature.

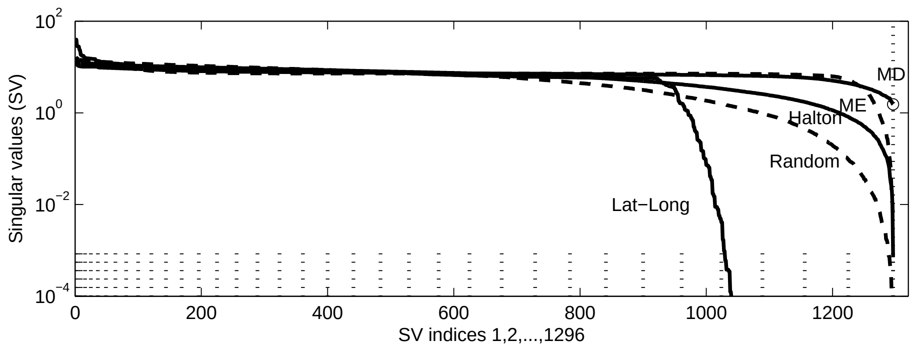

Fig. 4 The 1296 singular values for the SPH interpolation matrices in case of the five $N = 1296$ node point distributions shown in Figure 3. The dotted vertical line segments at the bottom of the figure indicate the number SPH modes present up through the successive SPH orders $0, 1\,2, \ldots, 35$.

last few singular values that are small. This suggests that direct SPH interpolation, as described in Section 2.1, may be improved by not interpolating with all SPH basis functions up through the maximal possible degree m (in case of $N = (m+1)^2$ nodes), but rather use least squares approximation based on lower degrees. The required change in the MATLAB code is minimal, with only one line of code affected. Instead of calling `inv(P)`, we can call `pinv(P(:,1:k*k))` to evaluate the *pseudoinverse* of the leading k^2 columns of the square $(m+1)^2 \times (m+1)^2$ matrix P, with $k = 1, 2, \ldots, m+1$. Just as before, the quadrature weights can then be read off from the first row of the resulting matrix. We will next see that $k = m$

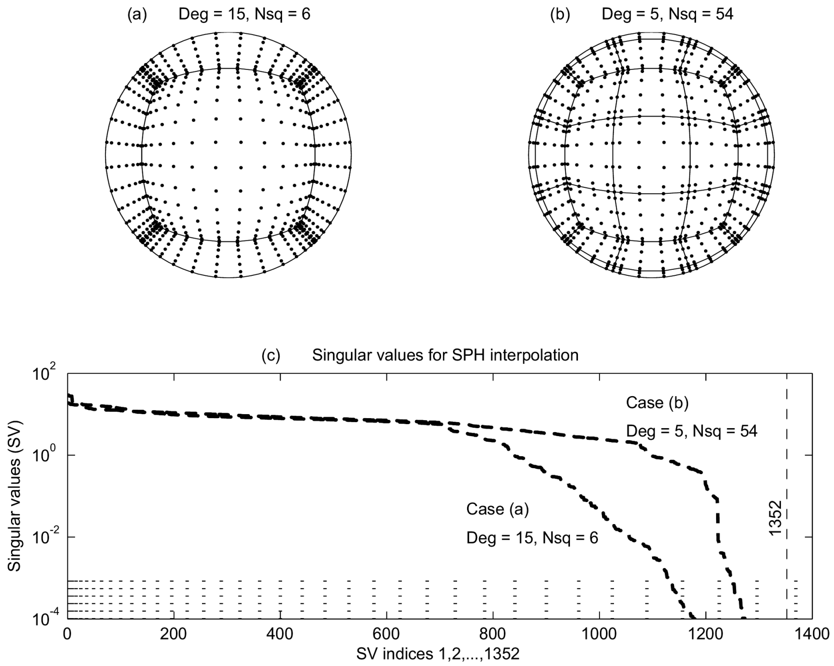

Fig. 5 Top row: Two examples of cubed sphere node sets, both with $N = 1352$ nodes, (a) degree 15 discretization over each of the Nsq = 6 faces of the cube, (b) each cube face is here divided in a 3×3 pattern of equal squares (with Nsq = 54 squares in all), using degree 5 discretization on each square, (c) the corresponding 1352 singular values in the two cases. A dashed vertical line marks the final SVD index 1352.

and $k = m - 1$ are very good choices in the case of ME nodes. The idea of using fewer SPH modes than node points has previously been considered in somewhat different quadrature contexts, c.f. Mhaskar et al. (2001) and Manuel et al. (2009).

4 Numerical test results

4.1 Test functions

Figure 6 illustrates three of the four test functions that were used in the present comparisons:

$$\begin{aligned}
f_1(x,y,z) &= 1 + x + y^2 + x^2 y + x^4 + y^5 + x^2 y^2 z^2 \\
f_2(x,y,z) &= 0.75\, e^{-(9x-2)^2/4-(9y-2)^2/4-(9z-2)^2/4} + \\
&\quad +0.75\, e^{-(9x+1)^2/49-(9y+1)/10-(9z+1)/10} + \\
&\quad +0.5\, e^{-(9x-7)^2/4-(9y-3)^2/4-(9z-5)^2/4} - \\
&\quad -0.2\, e^{-(9x-4)^2-(9y-7)^2-(9z-5)^2} \\
f_3(x,y,z) &= (1 + \tanh(-9x - 9y + 9z))/9 \\
f_4(x,y,z) &= (1 + \operatorname{sign}(-9x - 9y + 9z))/9\,.
\end{aligned} \tag{4}$$

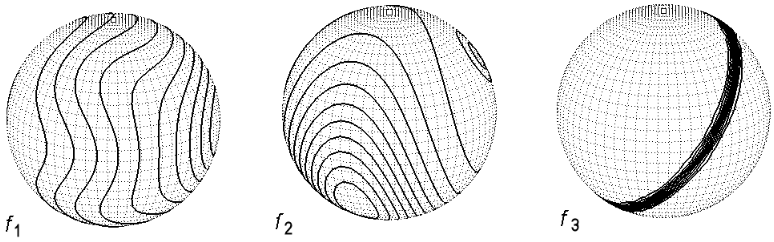

Fig. 6 The three test functions f_1, f_2, f_3 displayed by means of 10 equispaced contour lines. The fourth test function f_4 is very similar to f_3, but transitions discontinuously rather than steeply between the levels 2/9 and 0.

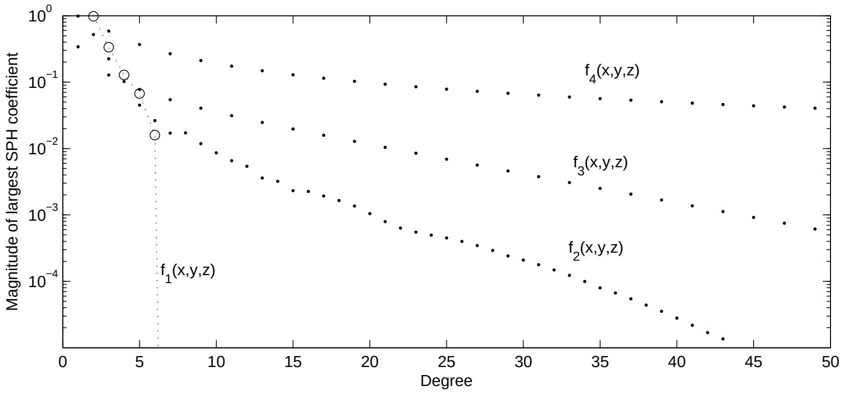

Fig. 7 Magnitude of largest (analytically calculated) SPH coefficient as function of its degree, shown for the four test functions. For the functions $f_3(x, y, z)$ and $f_4(x, y, z)$, only even degrees are visible since all odd degree coefficients vanish.

The first of these, $f_1(x, y, z)$, contains only SPH modes up through degree 6. The next two test functions have been considered repeatedly in the literature (Renka, 1988; Sommariva and Womersley, 2005). The function $f_2(x, y, z)$ is quite smooth, whereas $f_3(x, y, z)$ and $f_4(x, y, z)$ feature increasingly slowly converging SPH expansions, as illustrated in Figure 7. The surface integrals are

$$\begin{array}{ll} f_1(x,y,z): & 216\pi/35 \\ f_2(x,y,z): & 6.6961822200736179523\ldots \\ f_3(x,y,z): & 4\pi/9 \\ f_4(x,y,z): & 4\pi/9\ . \end{array} \tag{5}$$

4.2 Results with the present least squares approach

Figures 8-10 display test results for the first three functions f_1, f_2, f_3, respectively. In each case, results are shown for six different numbers of nodes: $N = 100$, 400, 1296, 1849, 3600, 6561. Each subplot displays four curves, one for each of the four node sets: MD (solid curve), ME (dashed curve), Halton (dash-dot curve) and Random (dotted curve). The horizontal axes show the highest order SPH included. The left edge represents using only the order zero degree SPH mode $Y_0^0(\underline{x}) \equiv \frac{1}{2\sqrt{\pi}}$, in which case all the quadrature weights become identical, $w_i = 4\pi/N$, independently of the node distribution. At the other extreme, the right edge represents using all the SPH modes, i.e. using interpolation rather than least squares when calculating the quadrature weights. The vertical axes show the worst quadrature error encountered in 1,000 separate tests, differing in that the node set (or equivalently, the test function) has undergone random 3-D rotations.

Comments on $f_1(x, y, z)$; Figure 8: In every case, errors fall to near machine accuracy whenever 6 or more SPH orders are included in the weights calculation. However, at the very far right - corresponding to calculating weights via SPH interpolation - a severe accuracy loss is seen in all but the MD case - consistent with the singular value situation seen in Figure 4.

Comments on $f_2(x, y, z)$; Figure 9: There now appears a clear distinction between the node sets, corresponding to their level of regularity, showing ME to perform the best and Random the worst. Omitting the highest SPH order(s) when calculating the weights is essential in all cases but for MD.

Comments on $f_3(x, y, z)$; Figure 10: This test function is less smooth still, but this makes no difference in the overall assessment. Especially for large N (high accuracy), the advantage of ME over MD becomes increasingly pronounced. Similar calculations with the discontinuous test function $f_4(x, y, z)$ shows further tendency towards increasing flattening of the curves, i.e. the corresponding subplots also become, for large N, reminiscent of the first two subplots in Figure 10.

4.3 Additional comparisons, also including Gaussian quadrature-type node/weight sets

4.3.1 Gaussian-type quadrature on the sphere

In 1-D, one needs data at N nodes in order to uniquely pin down a polynomial interpolant $p_{N-1}(x)$ of degree $N-1$. However, if the nodes are placed at certain Gaussian quadrature (GQ) locations, one can nevertheless obtain the exact quadrature results for all polynomials up through degree $2N-1$. The concept behind this is that the polynomial space that is not pinned down will have the property that all its members integrate to zero. The situation on the sphere is similar. Node locations can be found such that about $(m+1)^2/3$ nodes suffice to give the exact result for the first $(m+1)^2$ spherical harmonics (i.e. up through order m), c.f. McLaren (1963) and Ahrens and Beylkin (2009). The second of these references provide an algorithm for finding such node/weight sets.

4.3.2 The 'regularities' of the node and weight sets

The top right subplots in Figures 9 and 10 suggest that, in the case of $N = 1296$, suitable values for k (number on the horizontal axes, i.e. the maximal SPH degree

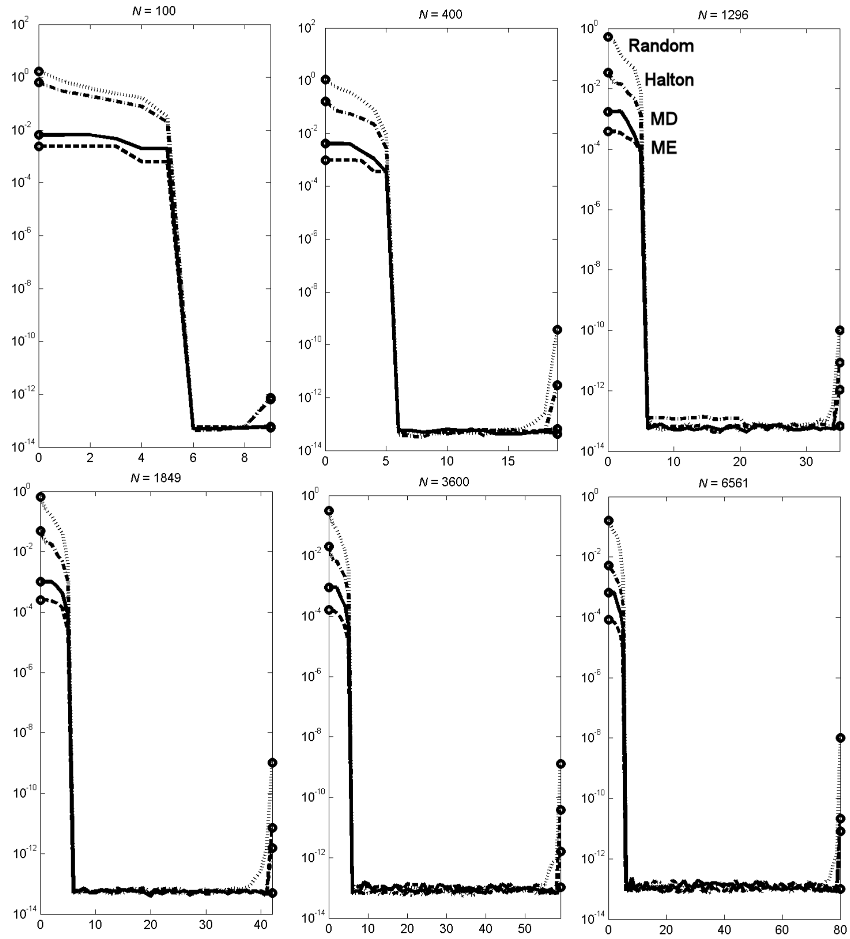

Fig. 8 Test results for $f_1(x, y, z)$: For each of six N-values, the worst error level encountered in 1,000 random node set rotations is displayed against the highest order of SPHs used in the weight calculation.

to include in the least squares process) would be

$$\begin{array}{lll} \text{Random} & 23 & \\ \text{Halton} & 31 & \\ \text{MD} & 35 & \text{(i.e. SPH interpolation)} \\ \text{ME} & 33 & \end{array} \tag{6}$$

Whether N is a perfect square or not, a simple rule of thumb for ME-like node sets is to fit with SPH functions about two degrees lower than the highest ones possible. This provides also a safe margin against accidental rank deficiencies. With the choices in (6), Figure 11 displays the obtained quadrature weight vs. the distance from the node to its nearest neighbor. Included also is a $N = 1332$

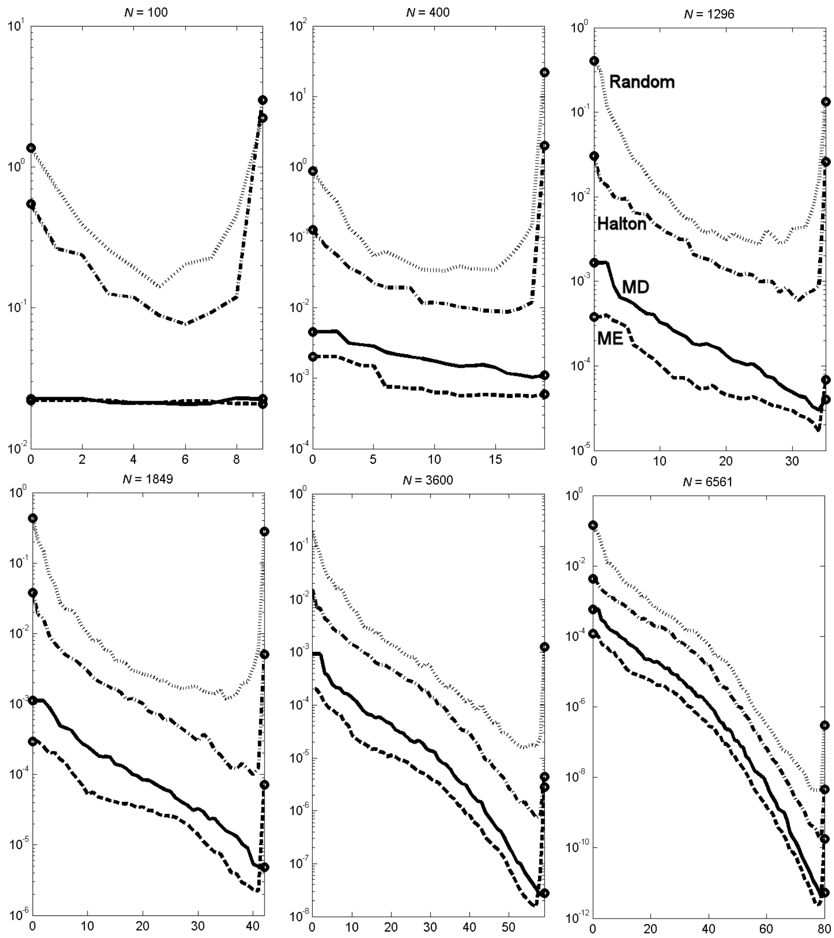

Fig. 9 Test results for $f_2(x, y, z)$: For each of six N-values, the worst error level encountered in 1,000 random node set rotations is displayed against the highest order of SPHs used in the weight calculation.

GQ set. The figure illustrates how irregularities in node distributions result in a corresponding scatter in the quadrature weights. Some more specific observations:

Halton and Random : The large scatter in the node distributions causes many weights to become negative. This is not altogether unreasonable, since best approximations over areas devoid of nodes would need to use derivative-like information from nearby nodes to best represent the integral over such areas.

MD, ME, and GQ : In the MD case, there is a very weak trend that nodes that are more distant from their surrounding ones get slightly larger weights. The ME nodes are (because of their construction) particularly uniform in terms of distances to nearest neighbors and thereby also in weights. If direct SPH interpolation was used for this same node set, the weights would become scattered irregularly between 0.0057 and 0.0135, reminiscent of the interpolation

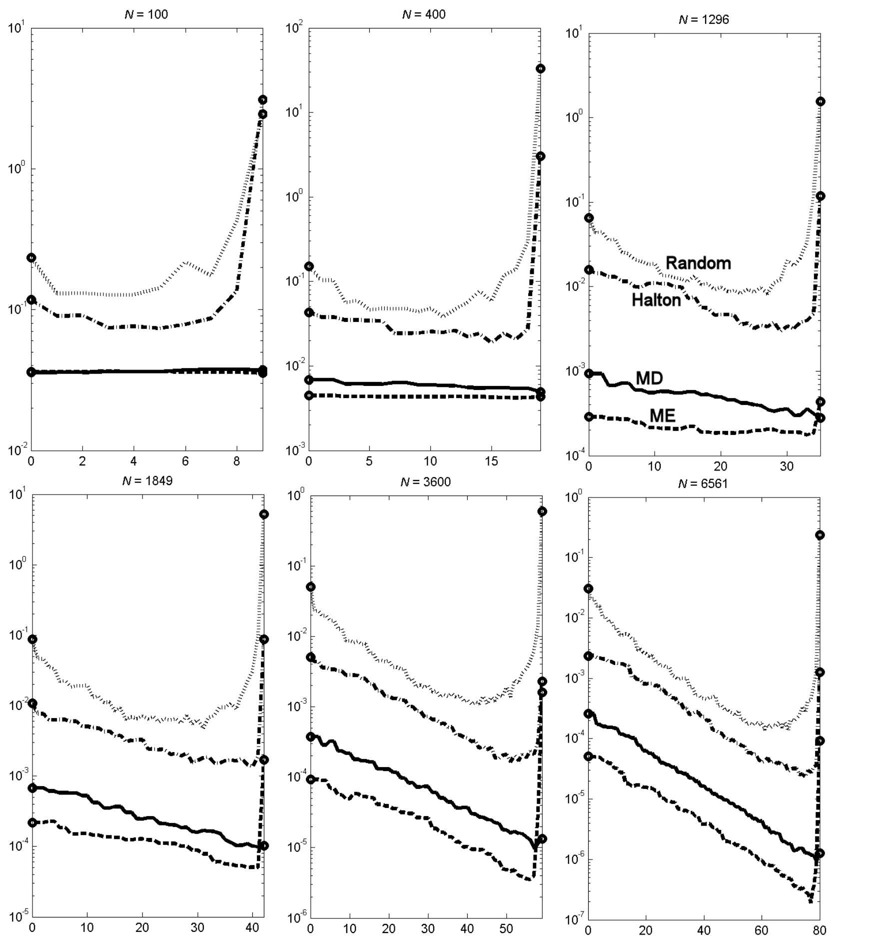

Fig. 10 Test results for $f_3(x, y, z)$: For each of six N-values, the worst error level encountered in 1,000 random node set rotations is displayed against the highest order of SPHs used in the weight calculation.

scatter seen in the lower subplot of Figure 2. The construction of the GQ set ensures again a very high level of weight uniformity in spite of its slightly larger variation in nearest-distances.

4.3.3 Accuracy comparisons

Figure 12 shows, separately for each of the test functions f_2, f_3, f_4, how the quadrature errors decrease with increasing node numbers when using the different node distributions and following the ad-hoc rule of thumb guidelines for choosing k as given in Section 4.3.2. In the case of the highly smooth test function f_2 (featuring a particularly rapidly convergent SPH expansion), the GQ approach is superior - not surprisingly since it integrates exactly about three times as many

SPH modes as there are nodes. With reduced smoothness of the test functions, the GQ advantage vanishes. A very similar situation is reported by Trefethen (2008), where 1-D GQ is compared against Clenshaw-Curtis integration. In most of our present cases, ME holds a small but distinct advantage over MD.

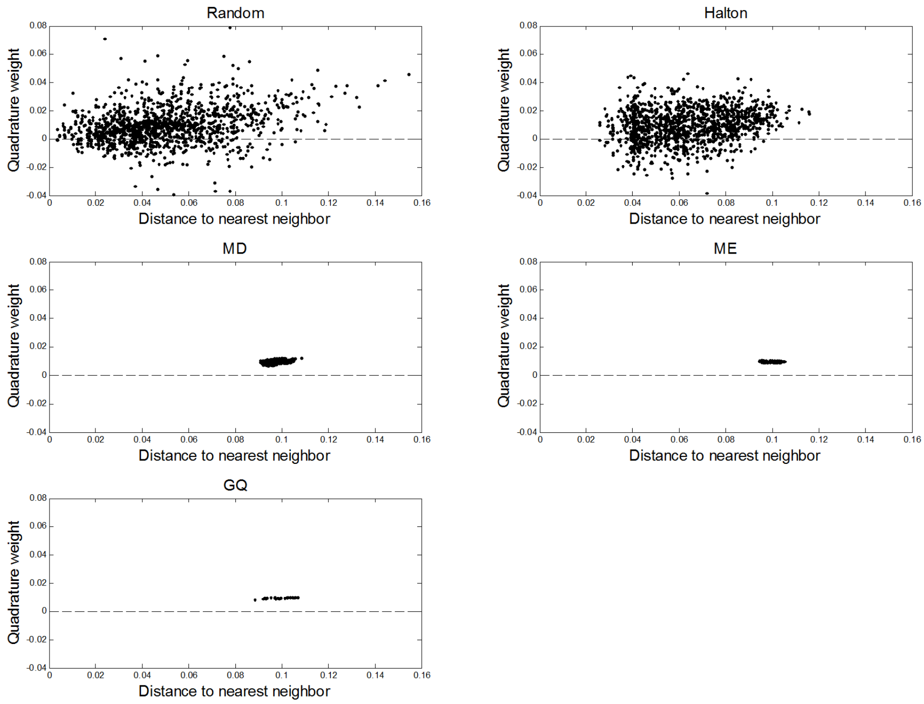

Fig. 11 The quadrature weight at a node plotted against the distance from the node to its nearest neighbor (in the case of $N = 1296$ nodes for Random, Halton, MD, ME; $N = 1332$ for GQ). All the five subplots have matching scales on their axes.

5 Conclusions

The test results and the discussion above show that, when integrating very smooth functions, the preference order between the node sets becomes GQ, ME, MD, followed somewhat distantly by the more irregular Halton and Random node sets. However, for functions of less smoothness (as would be typical for numerical PDE solutions obtained by RBF-FD methods), the differences become less pronounced, making ME a generally good and convenient choice. When calculating quadrature weights, it is for ME, Halton and Random nodes imperative to not use direct SPH interpolation, but to address the issue of small singular values and the associated rank deficiency. The proposed least squares approach - in MATLAB just changing `inv` to a `pinv` - provides a particularly simple approach for this.

The primary goals of the present study have been to improve the understanding of

SPH-based quadrature procedures and to minimize their sensitivity to details in the node distributions. Important further issues with regard to quadratures over a sphere include (i) finding weight sets for N nodes much faster than the present $\mathcal{O}(N^3)$ operations and (ii) finding good weight sets also for cases with very strong spatial variations in node density (as arises in applications utilizing local node refinements).

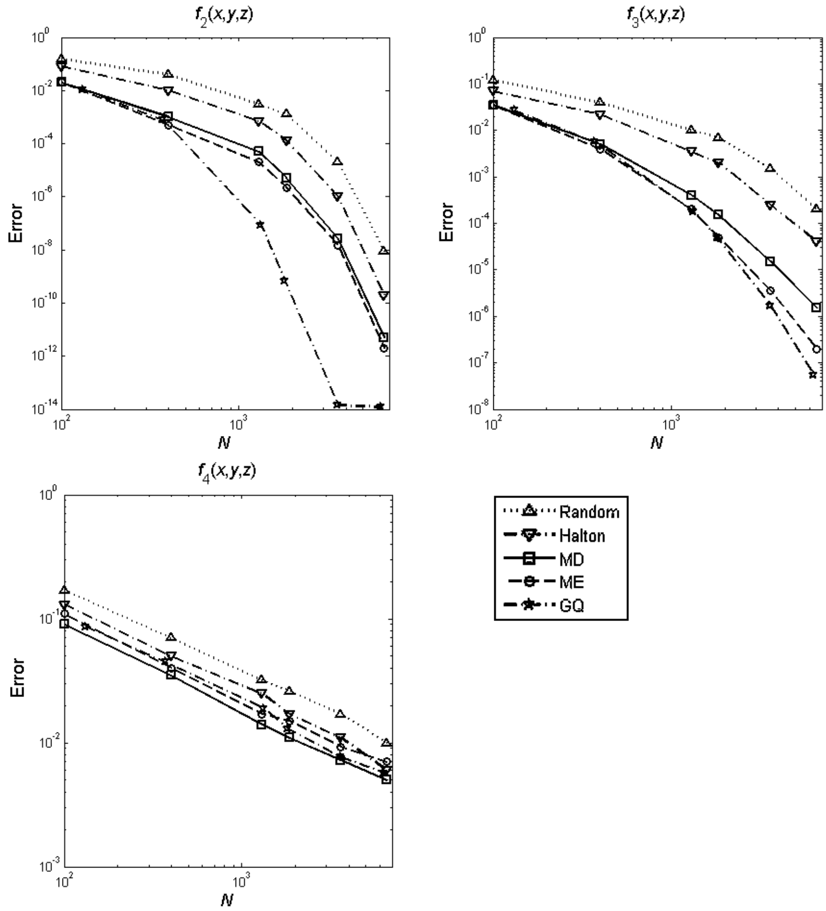

Fig. 12 The worst errors encountered when integrating 1,000 random rotations of the three test functions f_2, f_3, f_4 using quadrature based on five different node distribution strategies, in each case displayed against the number of nodes N.

Acknowledgements The present work was supported by the National Science Foundation grant DMS-0914647. Jessica Schmidt assisted in creating Figures 1 and 2. Prof. Gregory Beylkin provided us with node/weight sets for the GQ method described in Ahrens and Beylkin (2009). Discussions with Greg Barnett, Natasha Flyer, Erik Lehto and Brad Martin are also gratefully acknowledged.

References

C. Ahrens and G. Beylkin. Rotationally invariant quadratures for the sphere. *Proc. Roy. Soc. A*, 465:3103–3125, 2009.

J.P. Boyd. *Chebyshev and Fourier Spectral Methods.* Dover, New York, 2000.

P. C. Jr. Curtis. n-parameter families and best approximation. *Pacific J. Math.*, 93:1013–1027, 1959.

N. Flyer and B. Fornberg. Radial basis functions: Developments and applications to planetary scale flows. *Computers and Fluids*, 26:23–32, 2011.

N. Flyer, E. Lehto, S. Blaise, G. B. Wright, and A. St-Cyr. A guide to RBF-generated finite differences for nonlinear transport: Shallow water simulations on a sphere. *J. Comput. Phys*, 231:4078–4095, 2012.

N. Flyer, G.B. Wright, and B. Fornberg. Radial basis function generated finite differences: A mesh-free method for computational geosciences. In W. Freeden, M.Z. Nashed, and T. Sonar, editors, *Handbook of Geomathematics*, Berlin, 2014. Springer Verlag.

B. Fornberg and E. Lehto. Stabilization of RBF-generated finite difference methods for convective PDEs. *J. Comput. Phys.*, 230:2270–2285, 2011.

B. Fornberg and C. Piret. On choosing a radial basis function and a shape parameter when solving a convective PDE on a sphere. *J. Comput. Phys.*, 227: 2758–2780, 2008.

J. H. Halton. On the efficiency of certain quasi-random sequences of points in evaluating multi-dimensional integrals. *Numer. Math.*, 2(1):84–90, 1960.

K. Hesse, I. H. Sloan, and R. S. Womersley. Numerical integration on the sphere. In W. Freeden, M.Z. Nashed, and T. Sonar, editors, *Handbook of Geomathematics*, pages 1187–1219, Berlin, 2010. Springer Verlag.

J. C. Mairhuber. On Haar's theorem concerning Chebyshev approximation problems having unique solutions. *Proc. Amer. Math. Soc*, 7(4):609–615, 1956.

G. Manuel, S. Kunis, and D. Potts. On the computation of nonnegative quadrature weights on the sphere. *Appl. Comp. Harm. Anal.*, 27(1):124–132, 2009.

A.D. McLaren. Optimal numerical integration on a sphere. *Math. Comput.*, 17 (84):361–383, 1963.

H. Mhaskar, F. Narcowich, and J. Ward. Spherical Marcinkiewicz-Zygmund inequalities and positive quadrature. *Math. Comput.*, 70(235):1113–1130, 2001.

R.J. Renka. Multivariate interpolation of large sets of scattered data. *ACM Trans. Math. Software*, 14:139–148, 1988.

A. Sommariva and R. S. Womersley. Integration by RBF over the sphere. Applied Mathematics Report AMR 05/17, University of New South Wales, 2005.

L. N. Trefethen. Is Gauss quadrature better than Clenshaw-Curtis? *SIAM Review*, 50(1):67–87, 2008.

R. S. Womersley and I. H. Sloan. How good can polynomial interpolation on the sphere be? *Adv. Comput. Math.*, 23:195–226, 2001.

R. S. Womersley and I. H. Sloan. Interpolation and cubature on the sphere. 2003. http://web.maths.unsw.edu.au/ rsw/Sphere/.